

A mixed radial, angular, three-body distribution function as a tool for local structure characterization: Application to single-component structures

Supplementary Material

Sergey V. Sukhomlinov* and Martin H. Müser

Dept. of Materials Science and Engineering, Universität des Saarlandes, Saarbrücken, Germany

This supplementary information contains a visualization of the $\Sigma 5$ grain boundary in Sect. I and the radial distribution functions (RDF) $g(r)$ of all systems in Sect. II, for which the mixed radial, angular distribution function was shown in the main text of the article.

I. $\Sigma 5$ GRAIN BOUNDARY

Fig. S1(a) shows a unit cell used to simulate a double $\Sigma 5$ grain boundary in Al. The total number of atoms is $N = 2,460$. A view only on two atomic layers at the GB, perpendicular to the GB, is shown in Fig. S1(b).

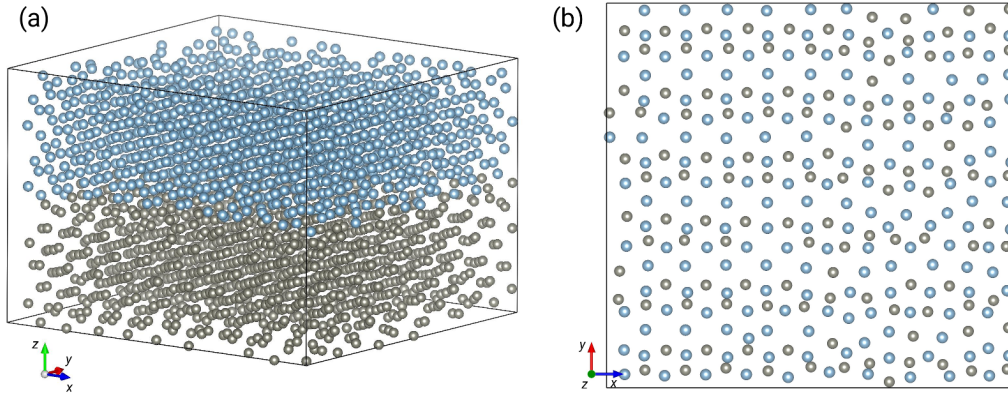


FIG. S1. An equilibrated snapshot of the $\Sigma 5$ -grain. Differently colored atoms belong to different grains. (a) The unit cell described in the main text is shown, (b) View of atoms belonging to two layers of the grain boundary.

II. RADIAL DISTRIBUTION FUNCTION

RDFs of face-centered cubic (Cu), hexagonal closed-packed (Mg), body-centered cubic (Na), pseudo-simple cubic (NaCl with all atoms treated as of the same type), face-centered cubic, namely A6 (In), diamond (Si), graphite (C) and rhombohedral, namely A7 (Sb), are presented in Fig. S2. The sequence of figures is consistent with the Fig. 2 of the main article. More details on the structures could be found in Sec. IIC of the main manuscript.

Fig. S3 shows the evolution of the radial distribution function along the Bain's path. 0% deformation corresponds to an ideal bcc structure, whereas 100% deformation - to an ideal fcc structure. Intermediate structures could be classified as bct or fct.

$g(r)$ of a $\Sigma 5$ grain boundary of Al at $T = 200$ K is presented in Fig. S4

Fig. S5 shows radial distribution functions of LJ melt at thermal energy of $k_B T = 0.708\varepsilon$ in subfigure (a), of LJ system quenched to $k_B T = 0.1\varepsilon$ in subfigure (b), as well as Cu melt at $T = 1,400$ K and Cu quenched to $T = 100$ K in subfigures (c) and (d), respectively.

* sergey.sukhomlinov@uni-saarland.de

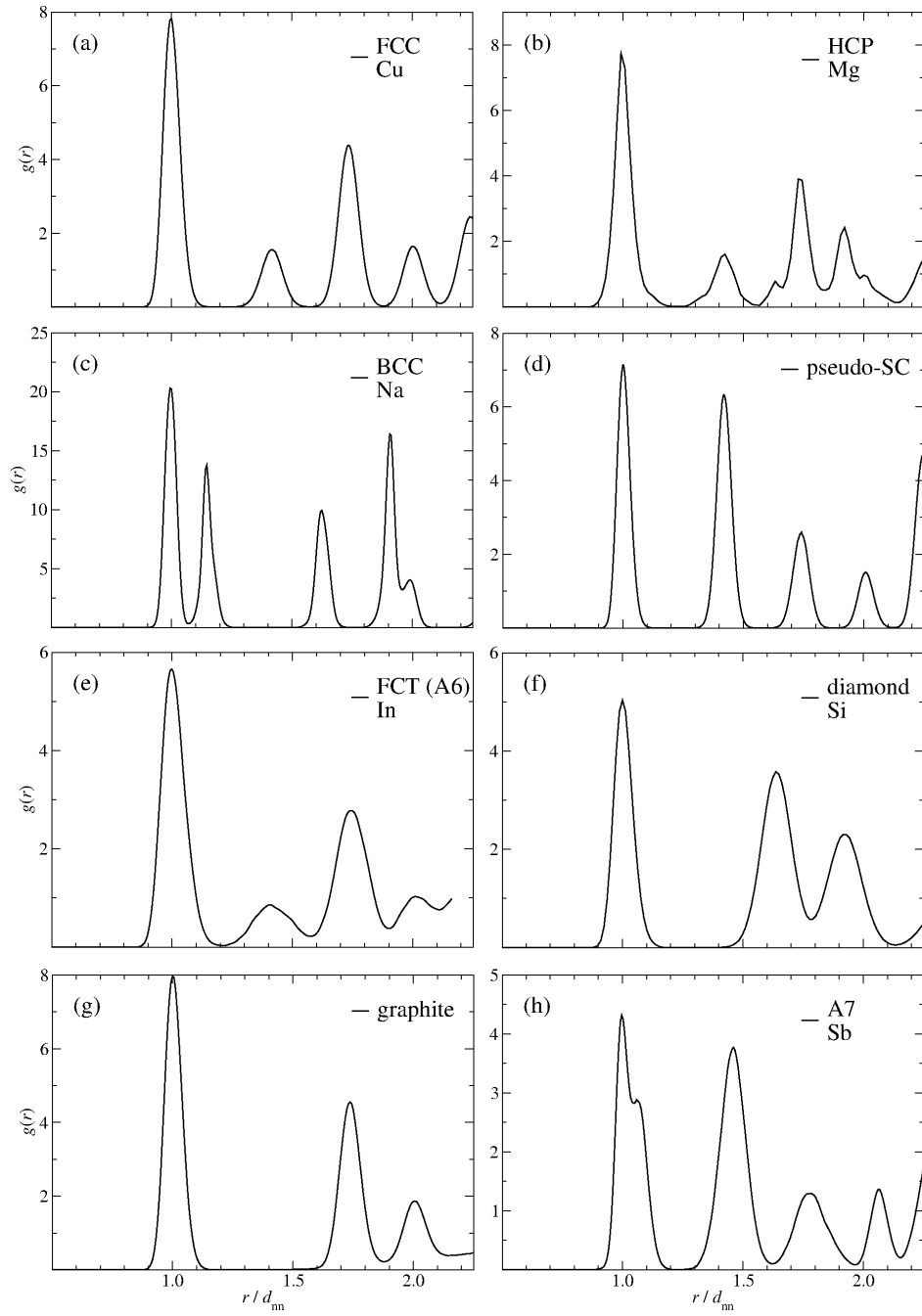


FIG. S2. $g(r)$ for the structures discussed in Sec. IIC of the main text. The sequence of sub-figures is consistent with the Fig. 2 of the paper. Distances are normalized to nearest-neighbor spacings. In sub-figure (d), all atoms in NaCl were treated as being identical. This produces $g(r)$ that is visually indistinguishable from that of a single-cubic (sc) structure – hence the name pseudo-sc.

Fig. S7 shows six radial distribution functions of silicon systems. In Fig. S7(a) and (b) we demonstrate $g(r)$ of diamond Si at $T = 1000$ K and of Si crystal with β -tin structure at $T = 300$ K, respectively. Subfigures (d) and (e) of Fig. S7 contain $g(r)$ of LDA Si and HDA Si, respectively. RDFs of tribo layer and of the intermediate-density silicon are shown in Fig. S7 (c) and (f), respectively. More details on these systems could be found in Sec. IIIC.

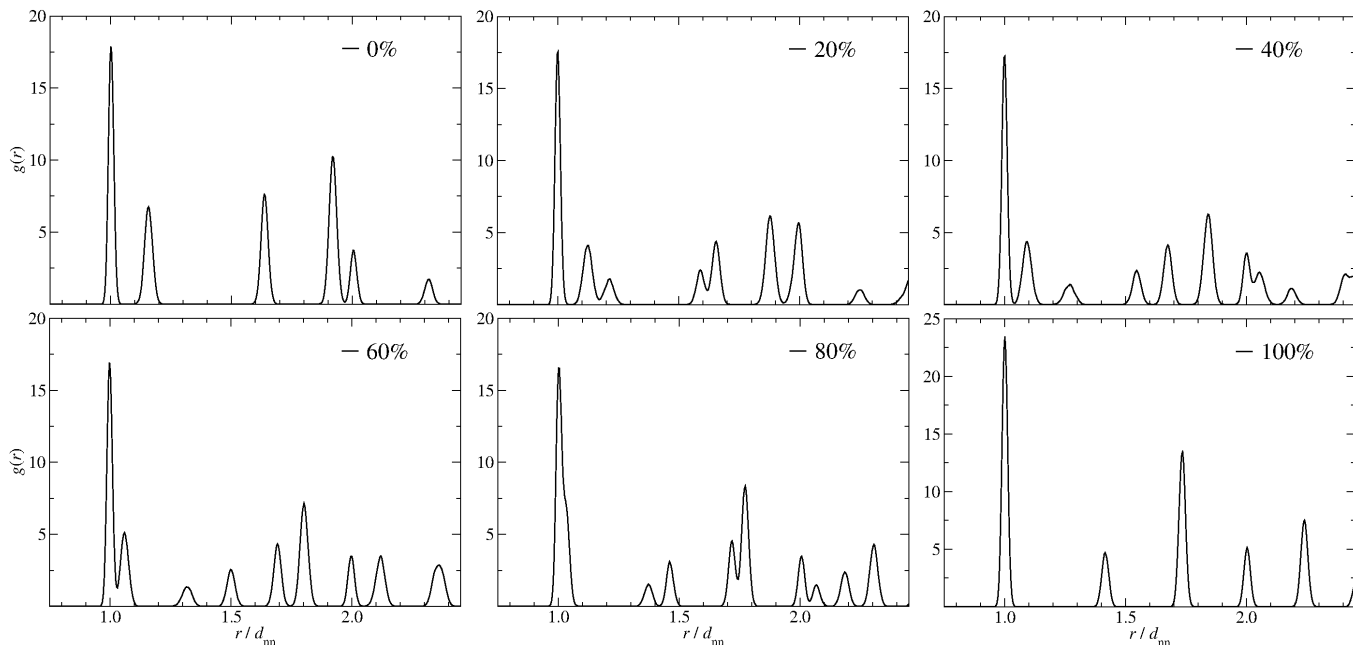


FIG. S3. $g(r)$ along the Bain's path. The starting structure is bcc and the gradual deformation along the Bain's path in percentages is given in the upper right corner of each graph. 0% corresponds to an ideal bcc structure, 100% - to an ideal fcc structure. The intermediate structures could be classified as bct (or fct). Distances are normalized to the pertinent nearest-neighbor spacing, which was estimated from the unit cell parameters. The sequence of sub-figures is consistent with the Fig. 3 of the paper.

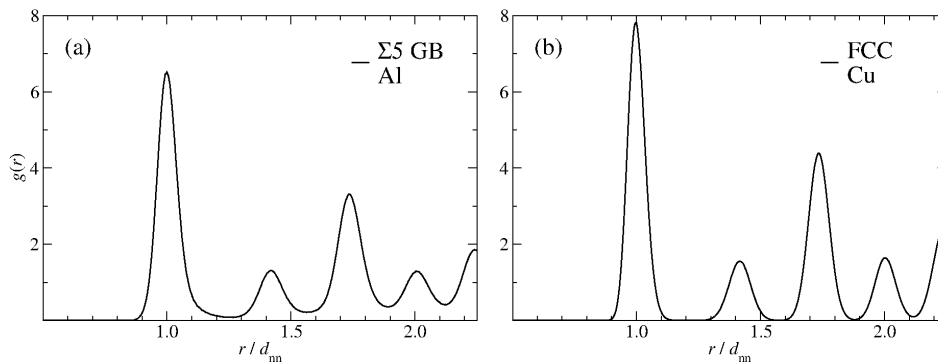


FIG. S4. $g(r)$ of (a) Al crystal with $\Sigma 5$ grain boundary at $T = 200$ K, and of (b) Cu crystal at $T = 300$ K. Distances are normalized to the pertinent nearest-neighbor spacings.

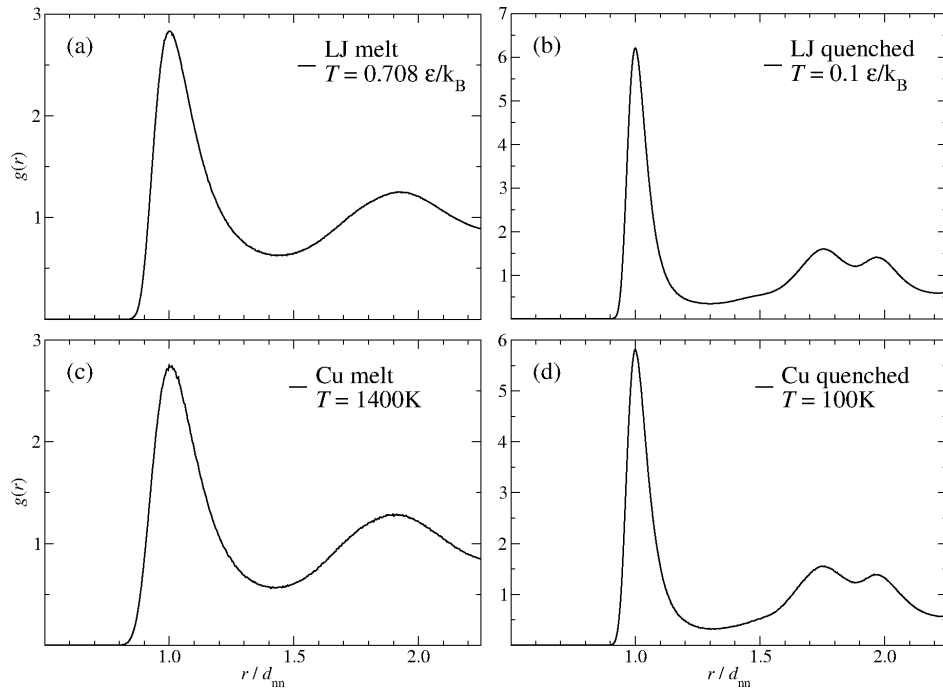


FIG. S5. $g(r)$ for Lennard-Jones system at (a) $k_B T = 0.708\epsilon$ in thermal equilibrium and (b) quenched to $k_B T = 0.1\epsilon$ as well as copper melt at (c) $T = 1,400\text{K}$ and (d) quenched to $T = 100\text{K}$. Distances are normalized to the pertinent nearest-neighbor spacing. The sequence of sub-figures is consistent with the Fig. 5 of the paper.

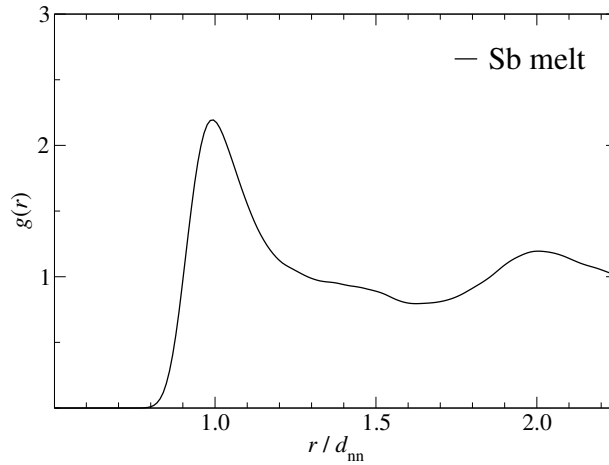


FIG. S6. $g(r)$ for liquid Sb at $T = 1100\text{K}$. Distances are normalized to the pertinent nearest-neighbor spacing.

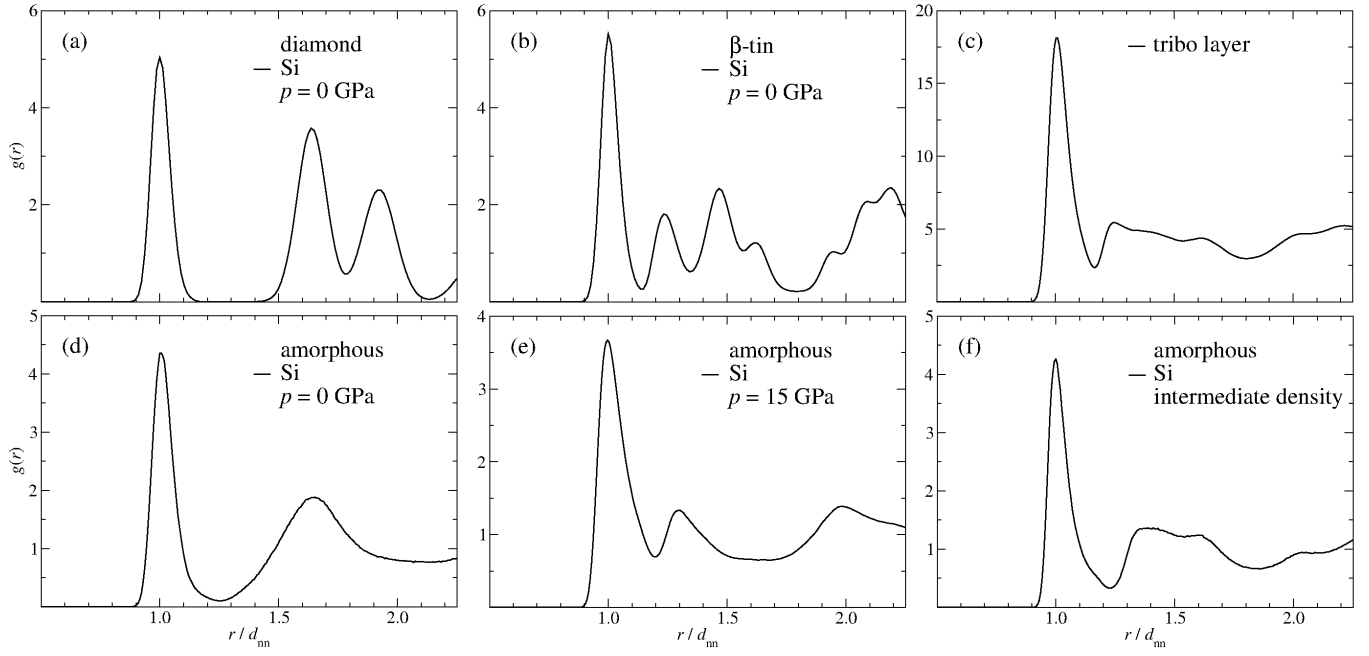


FIG. S7. $g(r)$ for (a) diamond Si structure, (b) β -tin structure of Si, (c) the amorphous Si obtained in a sliding experiment of two diamond blocks at external pressure of $p = 11$ GPa (see main text for more details), (d) amorphous Si at pressure $p = 0$ GPa, (e) amorphous Si at pressure $p = 15$ GPa, and (f) amorphous Si equilibrated at intermediate density (see main text for more details). Distances are normalized to the pertinent nearest-neighbor spacing. The sequence of sub-figures is consistent with the Fig. 7 of the paper.